LIMNOLOGY and OCEANOGRAPHY

ASLO

Limnol. Oceanogr. 9999, 2019, 1–12

doi: 10.1002/lno.11377

Mineral iron dissolution in *Trichodesmium* colonies: The role of O_2 and pH microenvironments

Meri Eichner [1*,a] **Subhajit Basu,** [2,3] **Siyuan Wang,** [2,3] **Dirk de Beer,** [1] **Yeala Shaked** [2,3]

[1]Max Planck Institute for Marine Microbiology, Bremen, Germany
[2]Interuniversity Institute for Marine Sciences, Eilat, Israel
[3]The Fredy and Nadine Herrmann Institute of Earth Sciences, Edmond J Safra Campus, Givat Ram, Hebrew University of Jerusalem, Jerusalem, Israel

Abstract

Colonies of the N_2-fixing cyanobacterium *Trichodesmium* can harbor distinct chemical microenvironments that may assist the colonies in acquiring mineral iron from dust. Here, we characterized O_2 and pH gradients in and around *Trichodesmium* colonies by microsensor measurements on > 170 colonies collected in the Gulf of Eilat over ~ 2 months. O_2 concentrations and pH values in the center of single colonies decreased in the dark due to respiration, reaching minimum values of 70 μmol L^{-1} and 7.7, whereas in the light, O_2 and pH increased due to photosynthesis, reaching maximum values of 410 μmol L^{-1} and 8.6. Addition of dust and bacteria and increasing colony size influenced O_2 and pH levels in the colonies, yet values remained within the range observed in single natural colonies. However, lower values down to 60 μmol L^{-1} O_2 and pH 7.5 were recorded in the dark in dense surface accumulations of *Trichodesmium*. Using radiolabelled ferrihydrite, we examined the effect of these conditions on mineral iron dissolution and availability to *Trichodesmium*. Dark-incubated colonies did not acquire iron from ferrihydrite faster than light-incubated colonies, indicating that the dark-induced decrease in pH and O_2 within single colonies is too small to significantly increase mineral iron bioavailability. Yet, ligand-promoted dissolution of ferrihydrite, a mechanism likely applied by *Trichodesmum* for acquiring mineral iron, did increase at the lower pH levels observed in surface accumulations. Thus, *Trichodesmium* surface blooms in their final stage may harbor chemical conditions that enhance the dissolution and bioavailability of mineral iron to the associated microbial community.

The bloom-forming cyanobacterium *Trichodesmium* is a globally important N_2 fixer estimated to contribute up to 50% of N_2 fixation in oligotrophic regions (e.g., Karl et al. 1997; Dore et al. 2002). Due to the high iron quota of the nitrogenase enzyme, N_2-fixing cyanobacteria such as *Trichodesmium* have a particularly high iron demand (Berman-Frank et al. 2001*a*). Consequently, N_2 fixation is often limited by iron availability on a global scale (e.g., Moore et al. 2009; Sohm et al. 2011).

At ambient pH and O_2 levels, solubility of iron is low, and the bulk of the iron pool is present as colloidal or particulate iron (Byrne and Kester 1976; Wu et al. 2001). The dissolution of iron from minerals generally requires protonation, reduction, or complexation by organic ligands (Schwertmann 1991). In contrast to many other phytoplankton types that rely on dissolved iron as their sole iron source, *Trichodesmium* has been shown to acquire iron from dust particles by accelerating the dissolution of mineral iron (Rubin et al. 2011; Basu and Shaked 2018). This ability to dissolve iron was linked to colony formation, as neither naturally occurring nor cultured single trichomes were able to dissolve iron from dust (Rubin et al. 2011). Such colony-specific mechanisms of iron acquisition might provide a benefit to colony formation that outbalances the negative impacts that O_2 accumulation during photosynthesis can have on N_2 fixation in colonies (Eichner et al. 2019*b*).

As part of their iron acquisition strategy, *Trichodesmium* colonies not only efficiently trap dust particles, but also actively move the particles to the colony center on the time scale of minutes to hours (Rubin et al. 2011). The physical proximity between particles and filaments optimizes the ability of the cells to internalize iron that dissolves from the mineral before it is lost by diffusion to the surrounding water (Basu et al. 2019). In addition to abiotic dissolution, the dissolution of mineral iron

*Correspondence: eichner@alga.cz

Additional Supporting Information may be found in the online version of this article.

[a]Present address: Centre Algatech, Institute of Microbiology of the Czech Academy of Sciences, Třeboň, Czech Republic

may be biologically enhanced in the colonies by reductive dissolution on the surface of *Trichodesmium* cells (Rubin et al. 2011) or by ligand-promoted dissolution (Basu et al. 2019). In the latter process, iron-specific ligands termed siderophores react with iron atoms at the mineral surface, followed by release of the iron-ligand complex into solution (Kraemer et al. 2005). *Trichodesmium* colonies in the Gulf of Eilat were recently shown to harbor a range of siderophore-producing bacteria (Basu et al. 2019; Gledhill et al. 2019), and addition of siderophores to natural colonies enhanced the dissolution as well as the uptake of mineral-bound iron by both *Trichodesmium* and associated bacteria (Basu et al. 2019). Taken together, these findings suggest that the close proximity of *Trichodesmium* cells, bacteria, and dust within colonies allows for efficient ligand-promoted dissolution and transfer of iron to *Trichodesmium* (Basu and Shaked 2018; Basu et al. 2019).

Another potential benefit of colony formation for iron acquisition is related to O_2 and pH gradients within colonies. Previous studies have demonstrated that photosynthesis and respiration by *Trichodesmium* can induce distinct O_2 and pH microenvironments within colonies (Paerl and Bebout 1988; Eichner et al. 2017, 2019*b*). Specifically, the decrease in pH levels and O_2 concentrations due to respiration in the dark may increase iron solubility (Breitbarth et al. 2010), enhance mineral iron dissolution rates (Millero et al. 2009), and subsequently increase iron availability to phytoplankton (Shi et al. 2010). The effect of pH on iron solubility involves changes in iron complexation by organic and inorganic ligands and redox reactions, and a slight increase in iron solubility is predicted until the end of the century due to the drop of 0.3 pH units under ocean acidification (Millero et al. 2009; Breitbarth et al. 2010). The dissolution rates of iron minerals can also be influenced by O_2 and pH via several pathways. First, naturally proton-promoted dissolution of mineral iron is accelerated by low pH (Schwertmann 1991; Morel and Hering 1993). Secondly, both ligand-promoted and reductive dissolution of mineral iron are pH-dependent, with low pH in the colony microenvironment potentially accelerating both the adsorption of ligands and/or reductant to the mineral surface and the subsequent release of Fe(III) or Fe(II) (Schwertmann 1991). Finally, lower O_2 concentrations in colonies might also increase iron availability by decreasing the rate of Fe(II) oxidation (Stumm and Lee 1961; Morel and Hering 1993).

Here, we investigated to what extent pH and O_2 microenvironments in *Trichodesmium* colonies affect the bioavailability of mineral iron. First, we characterized O_2 and pH gradients in a total of > 170 colonies collected in the Gulf of Eilat over a period of 2 months, covering a range of conditions, including, for example, different stages of a bloom, different colony morphologies, and different times of the diel cycle. In a second step, we aimed to predict the range of O_2 and pH conditions likely to occur in *Trichodesmium* microenvironments under conditions beyond those encountered during our field sampling, by systematically analyzing the effects of various parameters (colony size, dust, bacteria, and bloom formation) on colony microenvironments. Third, we determined the effects of these microenvironment conditions on mineral iron dissolution and its availability to *Trichodesmium*.

Material and methods

Colony sampling

Trichodesmium colonies were sampled in the Gulf of Eilat/Aqaba in the Red Sea over a period of 2 months from March to May 2018. Colonies were collected with a 200 μm net, either placed statically at ca. 1–2 m depth on a pole extended from the pier (3–4 m bottom depth) for approximately 2 h, or by vertical net tows from 20 m to the surface carried out from a boat at ca. 300 m bottom depth in the Gulf. Colonies were then hand-picked with Pasteur pipettes and washed in trace metal free, filtered seawater (cleaned using ion exchange resin Chelex 100).

Microsensor measurements

For microsensor measurements on single colonies, the colonies were placed in filtered seawater in plastic dishes of approximately 50 mL volume, and held in position with a thin glass needle above either a 1 cm layer of 0.5% agar or a nylon mesh to ensure unperturbed diffusion to all directions. Microsensor measurements on accumulations of colonies were performed in a measurement chamber shown in Supporting Information Fig. S1a, where colonies were concentrated in a small inner chamber of ca. 1 mL volume that was connected via a mesh at its bottom to an outer chamber with a larger volume of seawater (ca. 30 mL), aiming to simulate an aggregation of colonies at the sea surface that is in exchange with a larger body of water. Tuft-shaped colonies were added to the inner chamber at a concentration of ca. 40 ng chlorophyll *a* mL^{-1} (ca. 100 colonies mL^{-1} based on visual estimation). All measurements were performed at approximately 25°C and 350–450 μmol photons m^{-2} s^{-1}, unless specified otherwise.

Clark-type O_2 microelectrodes with a tip diameter of 10 μm were made and calibrated as described previously by Revsbech and Ward (1983). Microsensors for pH of 15 μm tip diameter were made as described previously by Kühl and Revsbech (2000). pH sensors were two-point calibrated with IUPAC buffers and values were subsequently corrected for variation in electrode performance assuming a pH of 8.2 in the bulk seawater surrounding the colonies (i.e., the average sea surface pH value at the sampling location and period according to Israeli National Monitoring Program [NMP, https://iui-eilat.huji.ac.il/Research/NMPAbout.aspx]). All pH values are reported on the NBS scale.

For recording depth profiles, microelectrodes were moved toward and through the colonies at 50–100 μm step size with a micromanipulator (VT-80, Micos) driven by a motor (Faulhaber minimotor, SA) while observing the colony at ca. ×5 magnification in a stereomicroscope (Nikon, SMZ1500

with camera Panasonic, DMC G5). Each colony was photographed for subsequent determination of colony dimensions. Volume and surface area were calculated assuming spherical geometry for puff-shaped colonies and ellipsoid geometry for tufts.

O_2 fluxes were calculated from the steady state O_2 gradients at the colony surface according to Fick's first law of diffusion:

$$J = -D(\Delta C/\Delta r) \quad (1)$$

where J represents the interfacial O_2 flux, D the diffusion coefficient for O_2 (2.2×10^{-9} m^2 s^{-1} at 25°C and salinity 40; Broecker and Peng 1974), and ΔC the concentration difference measured over the respective distance, Δr, at the colony surface. Interfacial flux was converted to the volume-normalized rate using estimates of surface area and volume for each colony. Fluxes were normalized to the inner core volume, with the surface of the core determined as the point of maximum gradient within the measured O_2 and pH gradients (cf. Fig. 1).

The theoretical O_2 uptake rate yielding anoxia at the center of the colony (i.e., diffusion-limited O_2 uptake) was calculated as a function of colony volume as described by Ploug et al. (1997). An apparent diffusivity of O_2 within the colony of 0.95x that of seawater (Ploug et al. 2008), a Sherwood number of 1 (i.e., no difference between the motion of the colony and that of the surrounding water, resulting in mass transfer merely by molecular diffusion but not advection), a bulk O_2 concentration of 212 μmol L^{-1} (i.e., air saturation), and a uniform respiration rate throughout the colony were assumed.

Experiments with isolated bacteria

For estimating the contribution of bacteria to the measured O_2 fluxes, two types of experiments with bacterial isolates were performed. Two strains (E6 and E23) isolated from *Trichodesmium* colonies in the Gulf of Eilat (Basu et al. 2019) were used. The culture suspension was washed three times in filtered seawater before use to eliminate potential toxic effects of bacterial exudates.

In the first set of experiments, O_2 profiles were measured on *Trichodesmium* colonies before and after addition of bacterial suspension to these colonies. The bacterial suspension was concentrated by centrifugation and 10–100 μL were pipetted onto individual *Trichodesmium* colonies placed in a small volume of seawater (50–100 μL) to maximize the physical contact between *Trichodesmium* and bacterial cells and retention of bacteria on the colony. Colonies were incubated with the added bacteria for 30–60 min before microsensor measurements. Cell concentrations in the bacterial suspensions were determined by cell counts on 4',6-diamidino-2-phenylindole (DAPI)-stained slides in a microscope (Nikon Eclipse Ci), yielding a total of ca. 1.2×10^7 (E23) and 0.7×10^7 (E6) cells added to each colony, respectively.

In a second set of experiments, O_2 profiles were measured on agar spheres containing the isolated bacteria. Agar spheres were prepared with seawater from the Gulf of Eilat amended with 0.5% agar, where the effective diffusion coefficient for O_2 is similar as in seawater (Ploug and Passow 2007). After dissolution of the agar, the solution was allowed to cool down to < 30°C, and mixed with bacterial suspension. Small amounts of food colorant were added to ease further handling. Spheres between 0.8

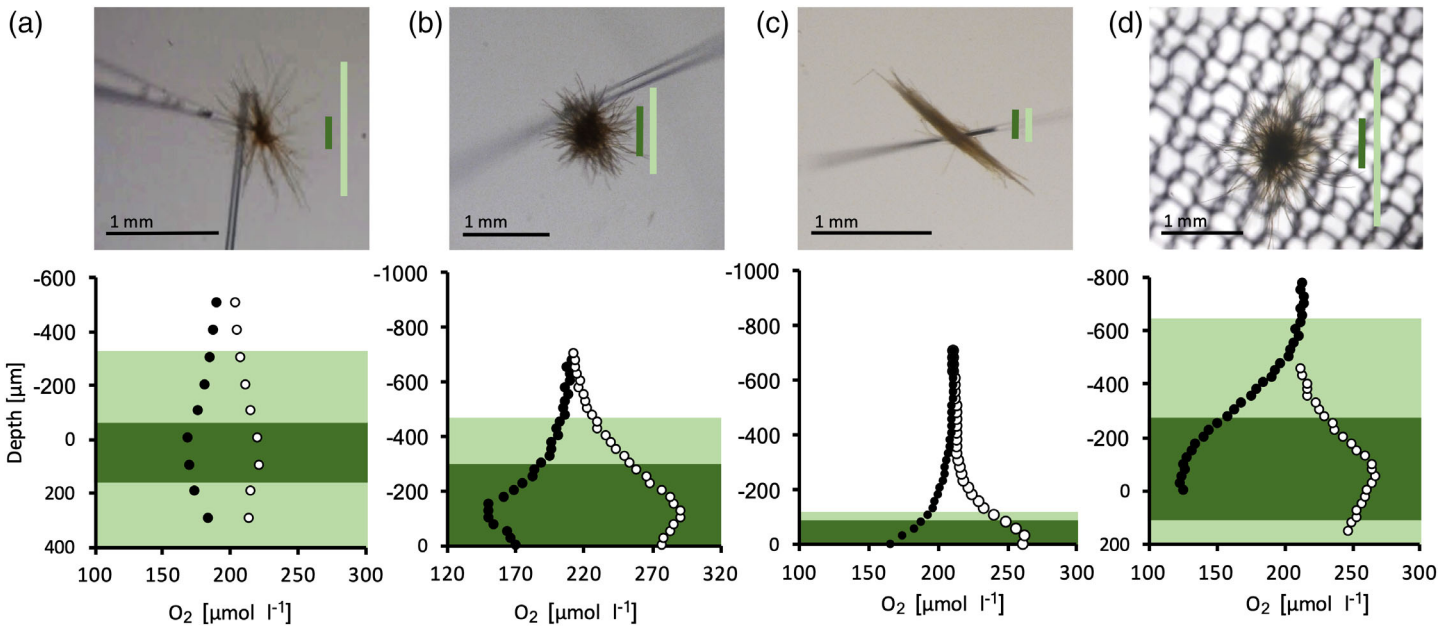

Fig. 1. (**a**–**d**): Typical morphology and depth profiles of O_2 measured in light (open circles) and dark (closed circles) for four different types of *Trichodesmium* colonies. Figure (**a**, **b**) shows two morphologically different types of puffs, figure (**c**) shows a tuft, and figure (**d**) shows an enlarged colony artificially produced by overnight incubation of several colonies at high density. Dark green bars in photos and dark green shading in depth profiles indicate the size and position of the colony core. Light green bars and shading indicate full colony size including trichomes extending outward from the core. Note figure (**a**) shows a microsensor approaching the colony.

and 2.3 mm diameter were produced by dripping small droplets of the bacterial agar suspension into seawater covered by a thin layer of oil (Ploug et al. 2002). The cell concentration in the bacterial suspension was determined by cell counts on DAPI-stained slides in a microscope (Nikon Eclipse Ci), yielding final concentrations of bacteria in the agar spheres of 1.34×10^{10} cells mL^{-1} (E23), 1.46×10^{10} cells mL^{-1} (E6), and 4.9×10^{9} cells mL^{-1} (E6 diluted). For microsensor measurements of O_2 profiles, the spheres were fixed with thin glass needles in the same setup used for *Trichodesmium* colonies.

Dust addition experiments

For dust addition experiments, a suspension containing approximately 2 mg L^{-1} of airborne dust collected in Eilat was applied to single colonies with an Eppendorf pipette. To minimize potential toxic effects of fast dissolving metals, the dust was washed three times in filtered seawater prior to usage.

Iron uptake assays

Rates of iron uptake from radioactively labeled ^{55}ferrihydrite colloids by natural colonies were determined as described previously by Basu and Shaked (2018). Briefly, 30–50 colonies were placed in small Petri dishes in 2 mL filtered seawater, at an irradiance of ca. 300 μmol photons m^{-2} s^{-1} and a temperature of ca. 25°C. ^{55}Ferrihydrite was pipetted directly onto the colonies, reaching a final concentration of 100 nmol L^{-1}. Four of the experiments (those on Mar 27th–29th) were conducted in the presence of 1 μmol L^{-1} of the siderophore desferrioxamine B (DFB). After 3–12 h, incubations were stopped by filtering colonies on 8 μm polycarbonate filters. Extracellular iron as well as attached bacteria were subsequently removed by a thorough wash in Ti-EDTA-citrate solution (as described by Basu and Shaked 2018) before determination of internalized ^{55}Fe (Tri-carb 1600 CA scintillation counter, Packard).

Abiotic dissolution experiments

Abiotic dissolution of radioactively labeled ^{55}ferrihydrite colloids under different pH levels was determined by monitoring the accumulation of dissolved ^{55}Fe over time. pH levels were adjusted with sodium hydroxide and hydrochloric acid and measured at the end of incubations with a pH electrode (Sentex). In order to estimate pH effects on ligand-promoted dissolution, incubations were performed in the presence of 2 μmol L^{-1} of the siderophore DFB. ^{55}Fe ferrihydrite colloids were incubated at a concentration of 200 nmol L^{-1}, and subsampled and filtered over 0.22 μm membrane filters (Millex GV, Merck) after incubation periods between 15 and 24 h, followed by determination of ^{55}Fe in the filtrate in a liquid scintillation counter (Tri-carb 1600 CA, Packard).

Results and discussion

O_2 and pH range in natural, single *Trichodesmium* colonies from the Gulf of Eilat

In the first set of experiments, O_2 and pH gradients in and around *Trichodesmium* colonies were determined by microsensor measurements on single, natural colonies. Distinct microenvironments were observed within colonies of different morphology, with O_2 concentrations and pH levels generally below air saturation in the dark due to respiration and above air saturation in the light due to photosynthesis (Fig. 1).

O_2 and pH microenvironments were highly variable between individual colonies (Fig. 2). Across all O_2 measurements on a total of 142 colonies, O_2 concentrations in the center of colonies ranged between 69 μmol L^{-1} (measured in the dark) and 412 μmol L^{-1} (measured in the light; Fig. 2). pH levels in the center of colonies (determined on a total of 36 colonies) ranged between 7.7 (measured in the dark) and 8.6 (measured in the light; Fig. 2). These measurements covered a range of different colony characteristics as well as sampling conditions over the 2-month sampling period, including a progressive rise in sea surface temperature along with an increase in stratification and decline in nutrient concentrations, a range of weather conditions, including a dust storm and flood (NMP, https://iui-eilat.huji.ac.il/Research/NMPAbout.aspx) and different sampling locations (ca. 10 m and ca. 300 m offshore) and depths (ca. 1–2 m and 0–20 m depth). Also individual colonies likely differed in nutrient status as suggested by measurements of alkaline phosphatase activity (data not shown) and observations of dust particles within the sampled colonies.

Both tuft- and puff-shaped colonies were sampled, with puffs dominating biomass for the major part of the sampling period and tufts dominating in the final week, when a *Trichodesmium* bloom characterized by patches of dense surface accumulations developed. Puffs differed significantly in the density of filaments with two distinct morphological types, one characterized by a small colony core relative to the total diameter (Fig. 1a) and a second, denser type, with a large colony core relative to the total diameter (Fig. 1b). O_2 concentrations and pH levels in the center of colonies were not significantly different between puffs and tufts (*t*-test, $p > 0.05$) or between the two puff morphologies (*t*-test, $p > 0.05$). Overall, the outer diameter of puffs ranged between 0.3 and 2.8 mm (1.1 ± 0.4 mm), while the inner core (cf. Fig. 1) ranged between 0.1 and 0.8 mm (0.3 ± 0.1 mm) in diameter.

Measurements were performed at different times of the day (Fig. 2a–d) to account for the physiological changes over the diel cycle observed previously in *Trichodesmium* (e.g., Berman-Frank et al. 2001*b*). When colonies were sampled and measured at nighttime, O_2 and pH levels were similar to those measured during the day under the respective light conditions (Fig. 2a–d).

Maximum range of microenvironment conditions expected in *Trichodesmium*

For a more systematic understanding of the potential effects of microenvironment conditions on mineral iron availability, we next estimated the extent of O_2 and pH deviations that could develop in *Trichodesmium* colonies under a range of different conditions beyond those captured during our sampling period. pH and O_2 conditions in the colony

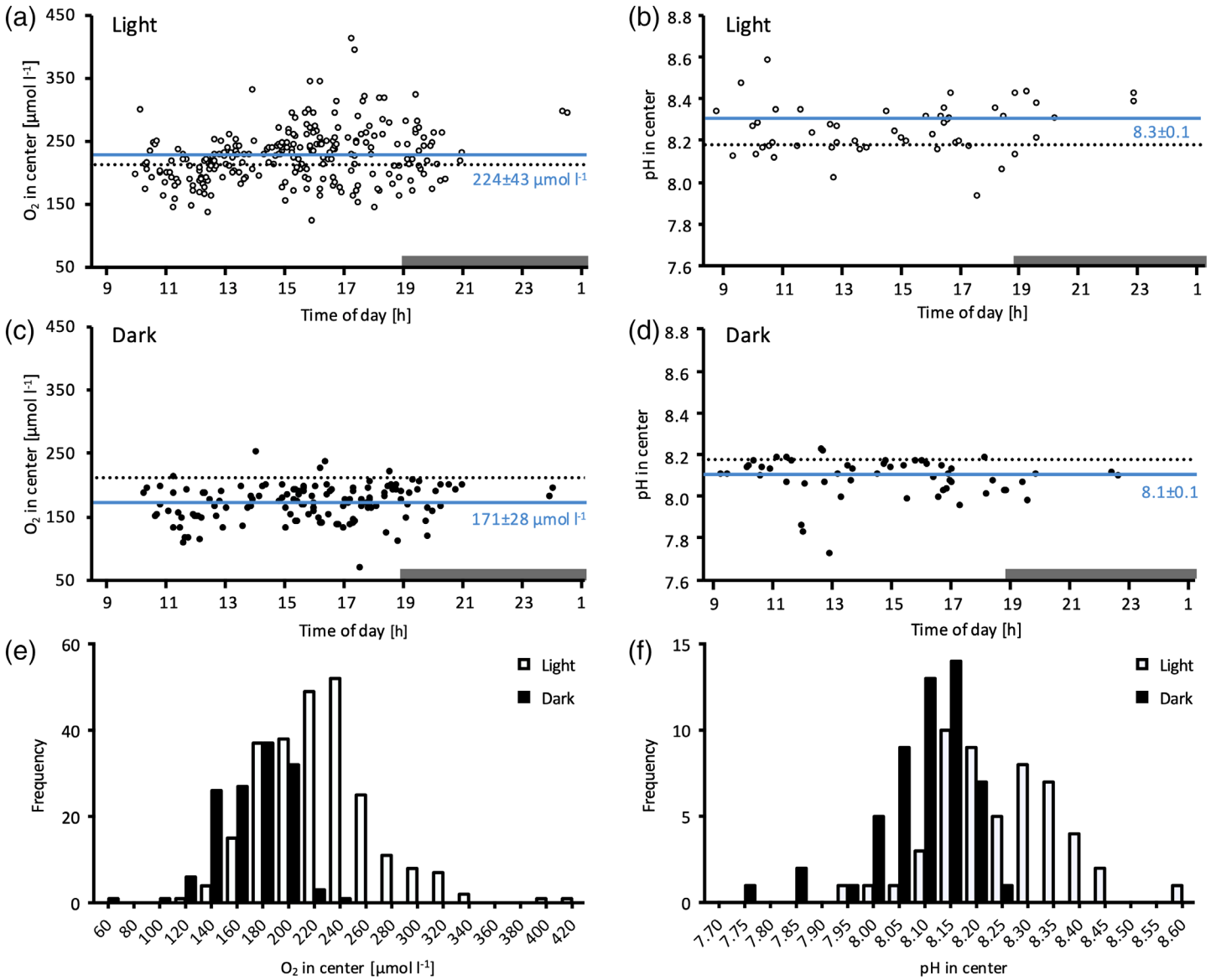

Fig. 2. O_2 (**a**, **c**, **e**) and pH (**b**, **d**, **f**) values measured in light (**a**, **b**) and dark (**c**, **d**) in the center of single *Trichodesmium* colonies sampled in the Gulf of Eilat. Figure (**a**–**d**) shows single measurements of O_2 or pH profiles performed at different times of the day. Average values are indicated by blue solid lines. Dotted lines indicate conditions in bulk seawater, gray bars on x-axes indicate period after sunset. Figure (**e**, **f**) shows the frequency distribution of O_2 and pH values in the center of colonies (pooled for all times of the day). Measurements were performed on a total of 142 and 36 colonies for O_2 and pH, respectively.

microenvironment are controlled not only by the rates of photosynthesis and respiration by *Trichodesmium*, but also by the metabolic activity of associated bacteria, potential chemical and physical effects of organic and inorganic material associated to the colonies, as well as colony size (e.g., Ploug et al. 2011; Klawonn et al. 2015). Hence, we characterized O_2 and pH microenvironments after modifying the amount of dust and the number of bacteria per colony as well as colony size. Additionally, we addressed whether the high density of *Trichodesmium* colonies during surface blooms induces microenvironments that are different from those in single colonies.

Effects of dust particles on O_2 and pH in colony microenvironments

In line with previous observations (Rubin et al. 2011), *Trichodesmium* colonies collected in this study often contained significant amounts of dust particles and were observed to actively move the dust to the center of the colony (Fig. 3). Here, we investigated whether the accumulation of dust particles and iron minerals in the colony center affects O_2 and pH microenvironments, either by chemical reactions associated to the dust particles or by changing the physical properties of the colonies (e.g., porosity). The effect of particles on pH and O_2

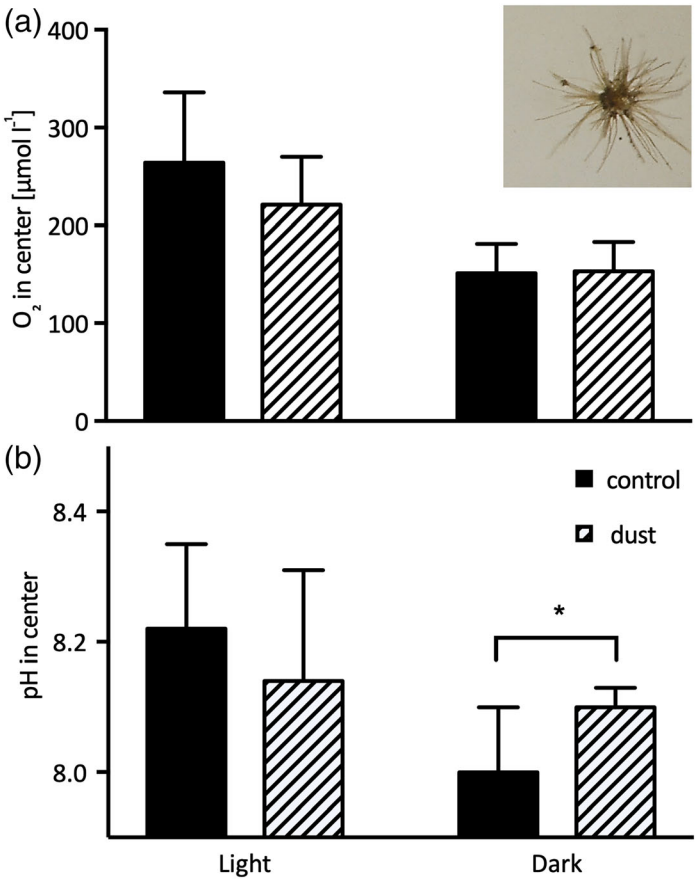

Fig. 3. O_2 (**a**) and pH (**b**) levels measured in the center of single *Trichodesmium* colonies before and after addition of dust particles. For O_2 $n = 8$, except for dust treatment in dark with $n = 6$. For pH $n = 3$. Asterisk indicates significant difference between dust treatment and control (*t*-test, $p < 0.05$). Inset shows an example of a *Trichodesmium* colony after addition of dust particles.

microenvironments was generally small, and in most cases not statistically significant (Fig. 3; Supporting Information Table S1). The most interesting observation with regards to the dust-amended colonies was that the pH remained unchanged when the colonies were photosynthesizing in the light or respiring in the dark, which was reflected in a significant increase in pH in the dark upon dust addition (Fig. 3b, $p < 0.05$). This buffering effect of dust on pH presumably results from dissolution of carbonate minerals present in the dust (e.g., Torfstein et al. 2017). The observation of dust buffering the respiration-induced drop in pH in the colony microenvironment is noteworthy and may bare implications for *Trichodesmium* blooms and surface accumulations, where association with dust may also minimize any decrease in pH during respiration.

Effect of associated bacteria on O_2 in colony microenvironments

Next, we tested to what extent respiration by bacteria associated with *Trichodesmium* can lower O_2 concentrations in the colonies. In a first approach, we added two different bacterial strains originally isolated from *Trichodesmium* in Eilat (Basu et al. 2019) to freshly collected colonies. While the initial abundance of (naturally occurring) bacteria in these colonies could not be quantified, we assumed a similar abundance as during a comparable sampling campaign at the same location ($7.5 \pm 0.46 \times 10^4$ cells colony^{-1}; Basu and Shaked 2018). The amount of bacteria ultimately incorporated into the colony after their addition and subsequent 30–60 min incubation likely depends on whether they preferentially resided in the colony microenvironment, which can be facilitated by motility and chemotactic behavior (e.g., Stocker and Seymour 2012). Accounting for the full range of potential behavior, we estimate that our manipulation resulted in at least a doubling of the bacterial abundance per colony (assuming homogenous distribution in the seawater containing the colony), and at most an increase by two orders of magnitude (assuming exclusive localization of bacteria in the colony microenvironment after the incubation). This increase in bacterial abundance did not yield consistent effects between experiments (Fig. 4a), yet, in all of the experiments, O_2 concentrations in the center of colonies remained above 167 μmol L^{-1} (Fig. 4a).

In a second, independent approach to estimate the effect of bacteria on colony microenvironments, we measured O_2 uptake in agar spheres containing different concentrations of the bacterial isolates. O_2 uptake rates in these agar spheres were positively correlated with bacterial density ($R^2 \geq 0.95$, Fig. 4b). Both bacterial strains and a more diluted culture of strain B6, all revealed a similar relationship (slope) between O_2 uptake rates and bacterial density, suggesting that these observations can be generalized (Fig. 4b). We hence applied the relationship between O_2 uptake rate and bacterial density that was determined in agar spheres to estimate the contribution of bacteria to total O_2 uptake by the colony consortium. Since the bacterial densities previously determined in *Trichodesmium* colonies from the Gulf of Eilat of $5–11 \times 10^4$ cells colony^{-1} (Basu and Shaked 2018) are below those tested in the agar sphere experiments (Fig. 4b), we extrapolated the bacterial O_2 uptake rates to naturally relevant bacterial densities (Fig. 4c). Comparing these extrapolated bacterial O_2 uptake rates with the average dark O_2 uptake by *Trichodesmium* colonies in this study (calculated according to Eq. 1) indicates that bacteria contribute less than 1% to the total O_2 uptake by natural *Trichodesmium* colony consortia (Fig. 4c). Our measurements of bacterial respiration rates in agar spheres thus suggest that natural variations in bacterial concentrations in *Trichodesmium* colonies are unlikely to induce major changes in O_2 microenvironments.

However, in natural colonies, bacteria may benefit from dissolved organic carbon and/or nitrogen released by *Trichodesmium* (e.g., Karl et al. 1992), which might stimulate their respiration rates compared to the agar spheres used in our study. In line with this, higher cellular respiration rates have been reported for bacteria associated to natural marine snow aggregates (0.3–3 fmol C cell^{-1} h^{-1}; Ploug et al. 1999), as opposed to 0.02 fmol O_2 cell^{-1} h^{-1}; this study). Multiplying

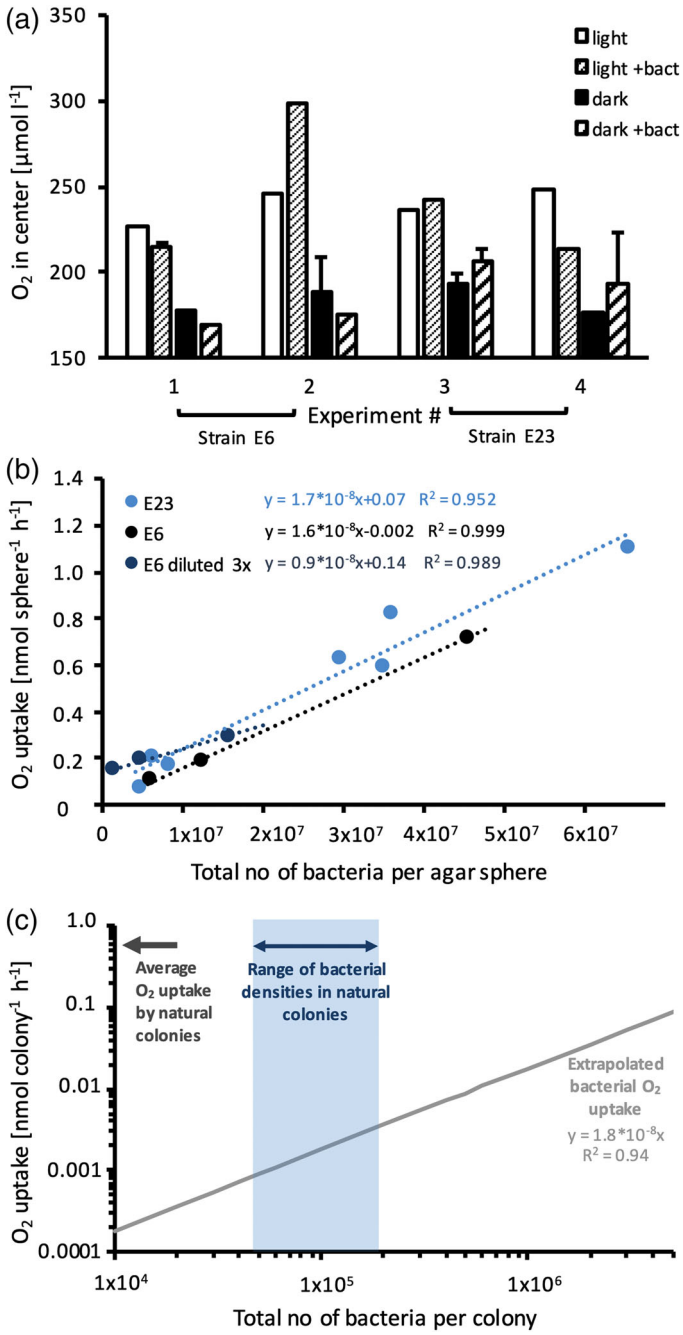

Fig. 4. (**a**) O_2 concentrations measured in the center of *Trichodesmium* colonies before and after addition of bacteria (+bact; resulting in a ca. twofold to 170fold increase of the number of bacteria per colony) in four different experiments, using two different bacterial isolates (strains E6 and E23). Error bars indicate standard deviation (SD) of 2–3 replicate measurements, data without error bars are single measurements. (**b**) O_2 uptake by bacteria isolated from *Trichodesmium* colonies, measured in agar spheres of different size, showing linear regression line for each bacterial isolate. (**c**) Estimated bacterial O_2 uptake at naturally relevant numbers of bacteria per colony, extrapolated from data shown in panel (**b**) (linear regression integrated for E23 and E6, with y-axis intercept set to 0). The range of bacterial densities observed in natural *Trichodesmium* colonies in Eilat (Basu and Shaked 2018) is indicated by blue shading. Average O_2 uptake by natural colonies measured in the dark (this study) is indicated by the arrow on the y-axis.

those estimates with the average bacterial abundance in *Trichodesmium* colonies determined by Basu and Shaked (2018) yields minimal and maximal bacterial respiration rates of 2.6×10^4 fmol O_2 colony^{-1} h^{-1} and 2.6×10^5 fmol O_2 colony^{-1} h^{-1}, respectively. Compared with the average colony consortium O_2 uptake rates in the dark of 5×10^5 fmol O_2 colony^{-1} h^{-1} measured here (Fig. 2), the lower estimate predicts only a small bacterial contribution to respiration ($\sim$ 5%), in general agreement with our data obtained on agar spheres (Fig. 4). However, the maximal estimate is in the same order of magnitude as O_2 uptake by the consortium measured here ($\sim$ 50%). Hence, we conclude that under conditions promoting high metabolic activity and abundance of associated bacteria, which may be more frequent in decaying colonies/blooms, O_2 concentrations within colonies may be significantly modified by bacterial respiration.

Effects of colony size on O_2 in colony microenvironments

In the next step, we investigated whether larger colony size could yield dark O_2 concentrations that were significantly lower than those determined in the natural colonies collected over the course of this study. To this end, we first measured O_2 uptake rates in colonies that were artificially enlarged by overnight incubation of several colonies at a high density. However, O_2 concentrations in these colonies in the dark, with average values of 140 ± 43 μmol L^{-1}, were only slightly lower than in natural puffs from the Gulf of Eilat (*t*-test, $p < 0.05$; Fig. 5a). Similarly, larger colonies collected in a previous study in the North Pacific Subtropical Gyre (NPSG; Eichner et al. 2017) did not show significantly lower O_2 concentrations in the dark (*t*-test, $p > 0.05$; Fig. 5a).

To investigate whether this lack of a size effect could be explained by diffusion limitation, we plotted O_2 uptake rates normalized to colony volume, and compared them to the theoretical diffusion-limited O_2 uptake rate, that is, the rate at which anoxia is reached exactly in the center of the colony (solid line in Fig. 5b; calculated according to Ploug et al. 1997). For the relatively small colonies sampled over the course of this experiment, size-normalized O_2 uptake rates were highly variable, suggesting that O_2 fluxes were controlled by other parameters rather than size, and O_2 uptake in most cases fell below the rates theoretically required for diffusion limitation/anoxia in the colony center by up to a factor of 100 (Fig. 5b). Also colonies from the NPSG and artificially enlarged colonies did not reach the rates required for anoxia (Fig. 5b). However, volume-normalized O_2 uptake rates in these larger colonies decreased with size, suggesting that a size-related factor other than O_2 diffusion, for example, diffusion of nutrients such as phosphorus into the colony, may indirectly control O_2 uptake in these colonies. By setting a boundary to the metabolic activity of *Trichodesmium* colonies, such a size-dependent limitation of nutrient uptake may prevent the development of anoxia in larger colonies. In conclusion, dust accumulation as well as higher bacterial numbers

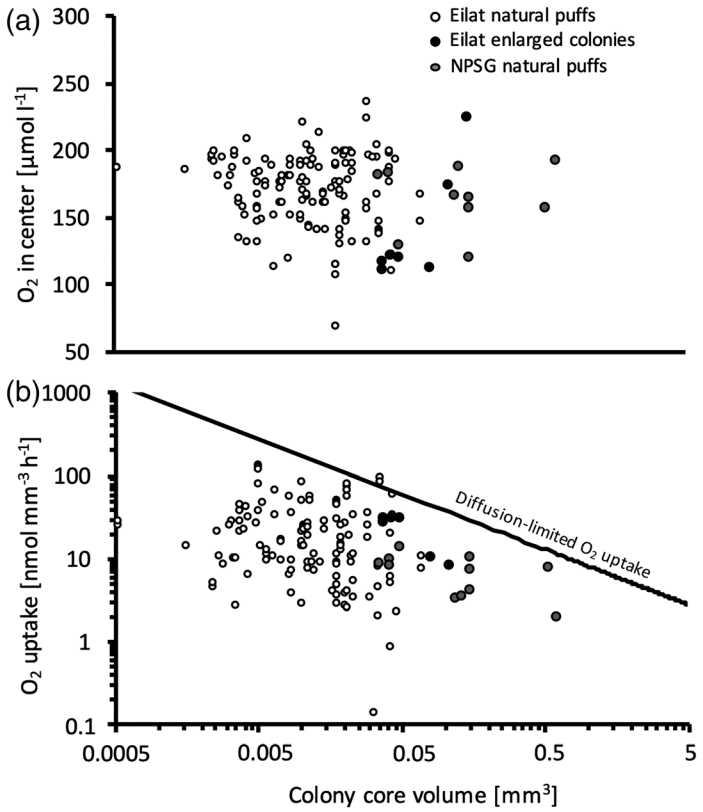

Fig. 5. O_2 concentrations in the center of colonies (**a**) and O_2 uptake rates (**b**) measured in the dark on *Trichodesmium* colonies of different sizes, including natural colonies collected in the Gulf of Eilat (this study, open circles), artificially enlarged colonies from the Gulf of Eilat (this study, black filled circles), and natural colonies collected in the NPSG (Eichner et al. 2017, gray filled circles). Solid line in (**b**) indicates the theoretical rate of O_2 uptake where O_2 fluxes become diffusion-limited and the center anoxic, calculated according to Ploug et al. (1997). Colony core volume was calculated based on the diameter of the dense colony core as indicated in Fig. 1.

and colony size could only moderately alter pH and O_2 levels in *Trichodesmium* colonies, suggesting that microenvironments reaching significantly beyond the conditions observed in single colonies over the course of our field sampling are unlikely to occur.

Effects of bloom formation on O_2 and pH microenvironments

As artificially increasing the size of single colonies did not substantially affect O_2 microenvironments (Table 1), we investigated in the next step whether accumulation of multiple colonies during a bloom might lead to O_2 and pH levels beyond the range observed in single colonies. Large numbers of single colonies often accumulate at the sea surface at the end of *Trichodesmium* blooms, forming a thin surface film of colonies. To investigate the effects of such surface accumulations on pH and O_2 microenvironments, we performed microsensor measurements on accumulations of tufts sampled during a naturally occurring bloom, which were brought to a similar density as in the field in a measurement chamber (Supporting Information Fig. S1a). O_2 and pH concentrations measured within these simulated blooms reached minimum pH levels and O_2 levels of 7.5 and 62 μmol L^{-1} in the dark, and maximum levels in the light of 382 μmol L^{-1} and 9.1 μmol L^{-1}, respectively (Table 1). It should be noted that in this setup, microsensors were not placed in the center of colonies, but between the surface of the tuft and the ambient seawater outside of the colony microenvironment. Hence, O_2 and pH levels in the center of tufts within a surface accumulation most likely reach more extreme values than those documented here. To illustrate the magnitude of this effect, we estimated the O_2 concentration in the center of a tuft under ambient O_2 concentrations observed in the bloom scenario (Supporting Information Fig. S1b) based on a typical O_2 gradient around a tuft (Fig. 1c), assuming that the rate of O_2 uptake is not dependent on the external O_2 concentration. For a tuft reaching ca. 170 μmol L^{-1} in the center as a single, free-floating tuft, this calculation suggests that in a surface accumulation, where average O_2 concentrations of ca. 150 μmol L^{-1} were measured, O_2 concentrations in the center of the tuft may range between 110 and 120 μmol L^{-1} (Supporting Information Fig. S1b). Applying an equivalent calculation to pH values yielded pH levels between 7.7 and 7.8 in the center of tufts at the average external pH measured in surface accumulations of colonies.

Effects of pH and O_2 microenvironments on dissolution and uptake of mineral iron

Effects of microenvironments on iron uptake from ferrihydrite

To determine whether the O_2 and pH microenvironments that develop in single colonies during photosynthesis and respiration affect the uptake of mineral iron by *Trichodesmium*, we compared iron uptake in light and dark in a total of 10 uptake experiments with natural colonies and ^{55}ferrihydrite (Fig. 6). Iron uptake rates per colony (143 ± 128 fmol colony^{-1} d^{-1}; Supporting Information Fig. S2) were in a similar range as in previous experiments (Basu and Shaked 2018). There was no consistent effect of light on iron uptake, with uptake in the light amounting to an average of $107\% \pm 51\%$ (n = 10) of uptake in dark across all experiments (Fig. 6). We conclude that the light-dependent changes in microenvironment conditions in single, naturally occurring *Trichodesmium* colonies collected over the course of our study were not strong enough to exert a significant effect on ferrihydrite bioavailability.

In four out of the 10 experiments, the rate of iron uptake by *Trichodesmium* strongly exceeded ferrihydrite dissolution rates measured in parallel in the absence of cells (Fig. 6). Since ferrihydrite is not internalized directly by *Trichodesmium* (Rubin et al. 2011), the surplus uptake over abiotic dissolution implies that *Trichodesmium* biologically enhanced ferrihydrite dissolution, in a process that may involve reductive and/or ligand-promoted dissolution, in agreement with previous reports by

Table 1. O_2 and pH values measured under different light conditions in natural, single *Trichodesmium* colonies and artificially enlarged colonies as well as in a surface accumulation of colonies. Note that values for single and enlarged colonies were measured in the colony center, whereas values for the surface accumulation were measured between accumulated colonies, close to their surface.

			O_2 (μmol L^{-1})	pH
Single natural colonies	Dark	Average ± SD	171 ± 28 (n = 143)	8.1 ± 0.1 (n = 53)
		Min	69	7.7
	400 μmol photons m^{-2} s^{-1}	Average ± SD	224 ± 43 (n = 251)	8.3 ± 0.1 (n = 52)
		Max	412	8.6
Enlarged colonies	Dark	Average ± SD	140 ± 43 (n = 7)	n.d.
		Min	110	n.d.
	400 μmol photons m^{-2} s^{-1}	Average ± SD	250 ± 75 (n = 6)	n.d.
		Max	381	n.d.
Surface accumulation of colonies	Dark	Average ± SD	149 ± 59 (n = 12)	7.9 ± 0.2 (n = 10)
		Min	62	7.5
	400 μmol photons m^{-2} s^{-1}	Average ± SD	193 ± 33 (n = 6)	8.4 ± 0.4 (n = 9)
		Max	237	9.1
	1000 μmol photons m^{-2} s^{-1}	Average ± SD	216 ± 99 (n = 8)	n.d.
		Max	382	n.d.

n.d., not determined.

Basu and Shaked (2018). Production of iron-binding ligands (siderophores) by the *Trichodesmium* consortium was recently documented in the Gulf of Eilat (Gledhill et al. 2019) and shown to increase ferrihydrite bioavailability by promoting its dissolution (Basu et al. 2019). To specifically test for microenvironment effects on ligand-promoted dissolution, four of the uptake experiments were conducted in the presence of the iron-binding ligand DFB (March 27th till March 29th; Fig. 6). In the remainder of the experiments, iron uptake was measured under natural conditions, allowing for reductive dissolution and self-dissolution in addition to ligand-promoted dissolution. As there was no systematic effect of light on iron uptake in either of these experiments, neither ligand-promoted nor reductive dissolution of mineral iron seemed to be affected by the light-dependent changes in microenvironment conditions in single colonies.

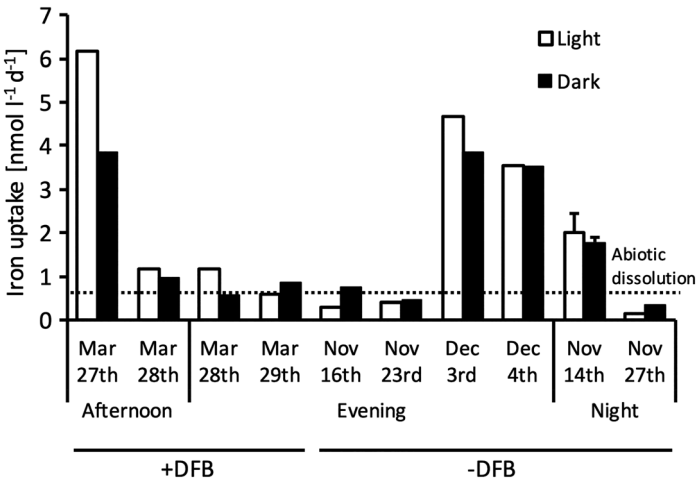

Fig. 6. Rates of iron uptake from ^{55}ferrihydrite by *Trichodesmium* colonies incubated in light and dark at different times of the day (afternoon between 11:30 h and 17:30 h; evening between 14:00 h and 22:40 h; night between 18:40 h and 08:40 h). Dotted line indicates the dissolution rate determined in controls without *Trichodesmium*. Experiments on March 27th–29th were conducted in the presence of 1 μmol l^{-1} of the siderophore DFB. Error bars for November 14th show SD of two replicate incubations, remaining data are single replicates containing 30–50 colonies each.

Results from a parallel study on the role of hydrogen microenvironments for iron acquisition suggested that the production of hydrogen during N_2 fixation may serve as an electron source for the reductive dissolution of mineral iron at the surface of *Trichodesmium* cells (Eichner et al. 2019*a*). While this pathway is indirectly affected by light due to its links to N_2 fixation and the photosynthetic/respiratory electron transport chain, net hydrogen evolution—and thus the potentially highest rates of reductive iron dissolution—was restricted to a relatively short period of the day when N_2 fixation was at its diel maximum (Eichner et al. 2019*a*), potentially explaining why light effects were not observed in the present study. Overall, these previous results suggested that the reductive dissolution of mineral iron may depend strongly on the diel patterns in *Trichodesmium* physiology. Here, we investigated the process of ligand-promoted iron dissolution in a simpler system, aiming to achieve a better mechanistic understanding of mineral iron dissolution in the colony microenvironment.

Effects of microenvironments on mineral iron dissolution

To test the effects of chemical microenvironments on ligand-promoted iron dissolution, we performed abiotic dissolution experiments with ferrihydrite and the siderophore DFB. Since our prediction of O_2 uptake rates under a range of conditions suggested that anoxia is unlikely to occur in *Trichodesmium* colonies, we focused on the effects of different pH levels. Ferrihydrite dissolution rates in the presence of DFB were increased by

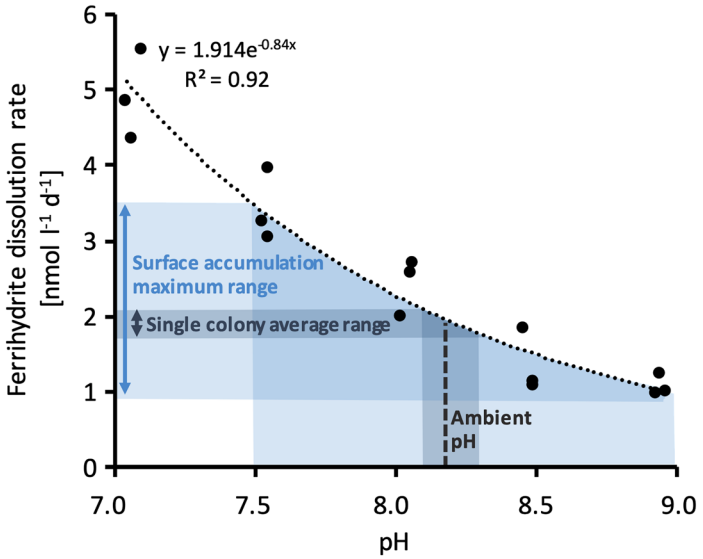

Fig. 7. Rates of abiotic dissolution of ferrihydrite at different pH levels measured in the presence of 2 μmol L^{-1} of the siderophore DFB to mimic ligand-promoted dissolution. Regression line shows exponential fit (R^2 = 0.92). Average pH range observed in the center of single *Trichodesmium* colonies and the respective predicted range of dissolution rates are indicated by dark blue shading and arrow on y-axis. Maximum pH range observed in surface accumulation of colonies and the respective predicted range of dissolution rates are indicated by light blue shading and arrow on y-axis. Dashed line indicates the average ambient pH based on monitoring data (NMP, https://iui-eilat.huji.ac.il/Research/NMPAbout.aspx).

approximately a factor of 5 at pH 7.0 compared to pH 9.0 (Fig. 7), demonstrating that ligand-promoted dissolution can indeed be enhanced by low pH levels. Considering the magnitude of this effect under the average pH variations observed in single, natural colonies (Table 1), however, confirms that those pH variations are not large enough to substantially affect ligand-promoted mineral iron dissolution, in line with the lack of light effects on iron uptake by natural colonies (Fig. 6). Ferrihydrite dissolution was altered by only 7% and 10% at the average pH level observed in the center of *Trichodesmium* colonies in the dark (pH 8.1) and light (pH 8.3), respectively, relative to the ambient pH level of 8.2 (Fig. 7). The small effect of pH on ferrihydrite dissolution and bioavailability is in line with a previous study by Shi et al. (2010), where a drop of ~ 0.6 pH units had a minimal effect on iron uptake rates from ferrihydrite by iron-limited diatoms.

However, at the lowest pH level observed across all measurements in this study, that is, pH 7.5 detected in dark in a surface accumulation of tufts (Table 1), the ferrihydrite dissolution rate was increased by ca. 80% relative to the rate at the ambient pH of 8.2 (Fig. 7). Hence, the availability of mineral iron liberated by ligand-promoted dissolution may be significantly increased when dense surface accumulations of colonies develop over the course of *Trichodesmium* blooms. It should be noted, however, that the high colony densities required to achieve pH deviations that are relevant for iron dissolution are often reached only at the end of the bloom, leaving little time for the *Trichodesmium* population itself to benefit from iron availability before the demise of the bloom. Yet, the microbial community associated to *Trichodesmium* may still be able to access the iron dissolved in these microenvironments. This way, colony microenvironments may increase the fraction of iron that remains in the microbial loop rather than sinking out of the water column in dust particles. As pH levels were also decreased in the seawater in the direct vicinity of colonies (Table 1), not only epibionts within colonies, but also microorganisms associated more loosely to the bloom might benefit from such elevated iron availability. Notably, this increase in iron availability will, however, only be a transient phenomenon occurring during the night or as decaying blooms sink to aphotic water layers, since elevated O_2 and pH levels caused by photosynthesis can hamper iron dissolution in the light. For instance, the highest pH level observed in the light (pH 9.1, Table 1) decreased ligand-promoted dissolution rates by ca. 50% relative to ambient pH (Fig. 7). Consequently, the diel changes in microenvironment conditions require a concerted diurnal coordination in the metabolism of *Trichodesmium* and its associated microbial community.

Conclusions

In summary, O_2 and pH deviations in single *Trichodesmium* colonies collected in the Gulf of Eilat were not strong enough to significantly affect the dissolution and uptake of mineral iron. The active centering and dissolution of dust particles in the colony core by *Trichodesmium* therefore seems to be unrelated to O_2 and pH gradients. Instead, the close proximity of *Trichodesmium* cells, dust particles, and associated bacteria in the colony core may benefit iron dissolution by reductive processes that are directly dependent on cell-surface contact, and/or by siderophores produced by associated bacteria (Rubin et al. 2011; Basu and Shaked 2018; Basu et al. 2019; Eichner et al. 2019*a*). Even though O_2 and pH microenvironments do not benefit iron acquisition in single *Trichodesmium* colonies, they may transiently enhance the supply of iron from dust to the associated microbial community in dense *Trichodesmium* blooms. This capacity of *Trichodesmium* blooms to modify the fate of mineral iron has potentially important implications for the ecosystem that may extend beyond the relatively short period of bloom events.

References

Basu, S., and Y. Shaked. 2018. Mineral iron utilization by natural and cultured *Trichodesmium* and associated bacteria. Limnol. Oceanogr. **63**: 2307–2320. doi:10.1002/lno.10939

Basu, S., M. Gledhill, D. de Beer, S. G. P. Matondkar, and Y. Shaked. 2019. Colonies of marine cyanobacteria *Trichodesmium* interact with associated bacteria to acquire iron from dust. Commun. Biol. **2**: 284. doi:10.1038/s42003-019-0534-z

Berman-Frank, I., J. T. Cullen, Y. Shaked, R. M. Sherrell, and P. G. Falkowski. 2001*a*. Iron availability, cellular iron quotas, and nitrogen fixation in *Trichodesmium*. Limnol. Oceanogr. **46**: 1249–1260. doi:10.4319/lo.2001.46.6.1249

Berman-Frank, I., P. Lundgren, Y. B. Chen, H. Küpper, Z. Kolber, B. Bergman, and P. Falkowski. 2001*b*. Segregation of nitrogen fixation and oxygenic photosynthesis in the marine cyanobacterium *Trichodesmium*. Science **294**: 1534–1537. doi:10.1126/science.1064082

Breitbarth, E., R. J. Bellerby, C. C. Neill, M. V. Ardelan, M. Meyerhöfer, E. Zöllner, P. Croot, and U. Riebesell. 2010. Ocean acidification affects iron speciation during a coastal seawater mesocosm experiment. Biogeosciences **7**: 1065–1073. doi:10.5194/bg-7-1065-2010

Broecker, W. S., and T. H. Peng. 1974. Gas exchange rates between air and sea. Tellus **26**: 21–35.

Byrne, R. H., and D. H. Kester. 1976. Solubility of hydrous ferric oxide and iron speciation in seawater. Mar. Chem. **4**: 255–274. doi:10.1016/0304-4203(76)90012-8

Dore, J. E., J. R. Brum, L. M. Tupas, and D. M. Karl. 2002. Seasonal and interannual variability in sources of nitrogen supporting export in the oligotrophic subtropical North Pacific Ocean. Limnol. Oceanogr. **47**: 1595–1607. doi:10.4319/lo.2002.47.6.1595

Eichner, M., and others. 2017. Chemical microenvironments and single-cell carbon and nitrogen uptake in field-collected colonies of *Trichodesmium* under different pCO_2. ISME J. **11**: 1305–1317. doi:10.1038/ismej.2017.15

Eichner, M., S. Basu, M. Gledhill, D. de Beer, and Y. Shaked. 2019*a*. Hydrogen dynamics in *Trichodesmium* colonies and their potential role in mineral iron acquisition. Front. Microbiol. **10**: 1565. doi:10.3389/fmicb.2019.01565

Eichner, M., S. Thoms, B. Rost, W. Mohr, S. Ahmerkamp, H. Ploug, M. M. Kuypers, and D. de Beer. 2019*b*. N_2 fixation in free-floating filaments of *Trichodesmium* is higher than in transiently suboxic colony microenvironments. New Phytol. **222**: 852–863. doi:10.1111/nph.15621

Gledhill, M., S. Basu, and Y. Shaked. 2019. Metallophores associated with *Trichodesmium erythraeum* colonies from the Gulf of Aqaba. Metallomics **11**: 1547–1557. doi:10.1039/C9MT00121B

Karl, D., R. Letelier, L. Tupas, J. Dore, J. Christian, and D. Hebel. 1997. The role of nitrogen fixation in biogeochemical cycling in the subtropical North Pacific Ocean. Nature **388**: 533–538. doi:10.1038/41474

Karl, D. M., R. Letelier, D. V. Hebel, D. F. Bird, and C. D. Winn. 1992. *Trichodesmium* blooms and new nitrogen in the North Pacific Gyre, p. 219–237. *In* E. J. Carpenter, D. G. Capone, and J. G. Rueter [eds.], Marine pelagic cyanobacteria: *Trichodesmium* and other Diazotrophs. Springer.

Klawonn, I., S. Bonaglia, V. Brüchert, and H. Ploug. 2015. Aerobic and anaerobic nitrogen transformation processes in N_2-fixing cyanobacterial aggregates. ISME J. **9**: 1456–1466. doi:10.1038/ismej.2014.232

Kraemer, S. M., A. Butler, P. Borer, and J. Cervini-Silva. 2005. Siderophores and the dissolution of iron-bearing minerals in marine systems. Rev. Mineral. Geochem. **59**: 53–84. doi:10.2138/rmg.2005.59.4

Kühl, M., and N. P. Revsbech. 2000. Biogeochemical microsensors for boundary layer studies, p. 180–210. *In* B. Boudreau and B. B. Jørgensen [eds.], The benthic boundary layer. Oxford Univ. Press.

Millero, F. J., R. Woosley, B. Ditrolio, and J. Waters. 2009. Effect of ocean acidification on the speciation of metals in seawater. Oceanography **22**: 72–85. doi:10.5670/oceanog.2009.98

Moore, C. M., and others. 2009. Large-scale distribution of Atlantic nitrogen fixation controlled by iron availability. Nat. Geosci. **2**: 867–871. doi:10.1038/ngeo667

Morel, F. M. M., and J. G. Hering. 1993. Principles and applications of aquatic chemistry. John Wiley & Sons.

Paerl, H. W., and B. M. Bebout. 1988. Direct measurement of O_2-depleted microzones in marine *Oscillatoria*: Relation to N_2 fixation. Science **241**: 442–445. doi:10.1126/science.241.4864.442

Ploug, H., M. Kühl, B. Buchholz-Cleven, and B. B. Jørgensen. 1997. Anoxic aggregates-an ephemeral phenomenon in the pelagic environment? Aquat. Microb. Ecol. **13**: 285–294. doi:10.3354/ame013285

Ploug, H., H. P. Grossart, F. Azam, and B. B. Jørgensen. 1999. Photosynthesis, respiration, and carbon turnover in sinking marine snow from surface waters of Southern California Bight: Implications for the carbon cycle in the ocean. Mar. Ecol. Prog. Ser. **179**: 1–11. doi:10.3354/meps179001

Ploug, H., S. Hietanen, and J. Kuparinen. 2002. Diffusion and advection within and around sinking, porous diatom aggregates. Limnol. Oceanogr. **47**: 1129–1136. doi:10.4319/lo.2002.47.4.1129

Ploug, H., and U. Passow. 2007. Direct measurement of diffusivity within diatom aggregates containing transparent exopolymer particles. Limnol. Oceanogr. **52**: 1–6. doi:10.4319/lo.2007.52.1.0001

Ploug, H., M. H. Iversen, and G. Fischer. 2008. Ballast, sinking velocity, and apparent diffusivity within marine snow and zooplankton fecal pellets: Implications for substrate turnover by attached bacteria. Limnol. Oceanogr. **53**: 1878–1886. doi:10.4319/lo.2008.53.5.1878

Ploug, H., B. Adam, N. Musat, T. Kalvelage, G. Lavik, D. Wolf-Gladrow, and M. M. Kuypers. 2011. Carbon, nitrogen and O_2 fluxes associated with the cyanobacterium *Nodularia spumigena* in the Baltic Sea. ISME J. **5**: 1549–1558. doi:10.1038/ismej.2011.20

Revsbech, N. P., and D. M. Ward. 1983. Oxygen microelectrode that is insensitive to medium chemical composition: Use in an acid microbial mat dominated by *Cyanidium caldarum*. Appl. Environ. Microbiol. **45**: 755–759.

Rubin, M., I. Berman-Frank, and Y. Shaked. 2011. Dust and mineral-iron utilization by the marine dinitrogen-fixer *Trichodesmium*. Nat. Geosci. **4**: 529–534. doi:10.1038/ngeo1181

Schwertmann, U. 1991. Solubility and dissolution of iron oxides. Plant Soil **130**: 1–25. doi:10.1007/BF00011851

Shi, D., Y. Xu, B. M. Hopkinson, and F. M. Morel. 2010. Effect of ocean acidification on iron availability to marine phytoplankton. Science **327**: 676–679. doi:10.1126/science.1183517

Sohm, J. A., E. A. Webb, and D. G. Capone. 2011. Emerging patterns of marine nitrogen fixation. Nat. Rev. Microbiol. **9**: 499–508. doi:10.1038/nrmicro2594

Stocker, R., and J. R. Seymour. 2012. Ecology and physics of bacterial chemotaxis in the ocean. Microbiol. Mol. Biol. Rev. **76**: 792–812. doi:10.1128/MMBR.00029-12

Stumm, W., and G. F. Lee. 1961. Oxygenation of ferrous iron. Ind. Eng. Chem. **53**: 143–146. doi:10.1021/ie50614a030

Torfstein, A., and others. 2017. Chemical characterization of atmospheric dust from a weekly time series in the north Red Sea between 2006 and 2010. Geochim. Cosmochim. Acta **211**: 373–393. doi:10.1016/j.gca.2017.06.007

Wu, J., E. Boyle, W. Sunda, and L. S. Wen. 2001. Soluble and colloidal iron in the oligotrophic North Atlantic and North Pacific. Science **293**: 847–849. doi:10.1126/science.1059251

Acknowledgments

We are grateful to Murielle Dray for technical assistance at IUI and to Yitzhak Jacobson for help with colony sampling. We also thank MPI staff Gabriele Eickert-Grötzschel, Ines Schroeder, Anja Niclas, Cäcilia Wigand, Vera Hübner, and Karin Hohmann for producing the microsensors, as well as Volker Meyer, Harald Osmers, and Paul Färber for their technical support with the associated equipment. This study was supported in part by Israel Science Foundation grant 458/15 (www.isf.org.il) and German-Israeli Foundation for Scientific Research and Development grant 1349 (www.GIF.org.il) awarded to Y.S. Additional funding was provided by the Minerva Foundation (M.E.), CSC-HUJI (S.W.), and the Max Planck Society.

Conflict of Interest

None declared.

Submitted 01 March 2019
Revised 13 August 2019
Accepted 02 October 2019

Associate editor: Anya Waite